Finite element modeling of rheological objects for simultaneously reproducing their deformation and force behaviors

Zhongkui Wang and Shinichi Hirai
Department of Robotics, Ritsumeikan University
Noji-higashi 1-1-1, Kusatsu, 525-8577, Japan
gr046074@ed.ritsumei.ac.jp, hirai@se.ritsumei.ac.jp

***Abstract*— Among modeling of deformable objects, such as human organs or tissues, various food products, and cloth, accurate reproduction of rheological properties is a challenging issue because rheological objects always yield residual deformation after arbitrary operations. In this paper, a finite element (FE) model was presented to simulate rheological behaviors. In order to reproduce both deformation and force behaviors simultaneously, two sets of physical parameters were estimated based on the FE model and nonlinear optimization. A parameter switching strategy was then proposed to switch the parameters from one set to the other during simulation. Experimental results of commercial clay and Japanese sweets material were presented to validate our FE model for simultaneous reproduction of rheological deformation and force behaviors. Contact simulations between rheological objects and external instruments were also presented to shown the ability of our FE model for dealing with arbitrary shaped objects.**

I. INTRODUCTION

Modeling of deformable objects, such as human organs or tissues, various food products, and cloth, has been studied for over twenty years [1], [2]. In our definition, deformable objects was roughly divided into three categories based on their deformation behaviors: elastic, plastic, and rheological object. Elastic or viscoelastic objects have the ability to completely recover the deformations generated during operations and plastic objects completely maintained those deformations. Rheological objects, on the other hand, have both elastic and plastic properties. The deformation generated in rheological objects was partially recovered and partially maintained.

Modeling of elastic or viscoelastic objects has been studied intensively, especially in surgical related applications since most biological organs and tissues seem to be recoverable. Some organs or tissues, however, may fail to completely recover from the deformation. Porcine brain tissue was found to be one example [3]. In vivo experimental results also showed residual deformation presented in human liver [4]. In addition, many other objects, such as clay and various food products, demonstrate rheological behaviors. However, modeling and property estimation of rheological objects was not studied sufficiently until now. Chua *et al*. has stated that the most critical barrier against the application of robotics and automation in food industry is a lack of understanding of the food product properties as an "engineering" material for handling operations [5].

Early work on the modeling of rheological objects dates back to Terzopoulos *et al*. [2], who has used a Burgers model to describe rheological behaviors. However, it is only a conceptual description and no simulation results and parameter information were given. A mass-spring-damper (MSD) model was introduced to model a food dough and the physical property was calibrated by genetic algorithm (GA) optimization [6], [7]. The MSD model has an advantage of less computation costs [8], but the formulation was not based on continuum mechanics and the simulation accuracy is quite limited. A two-layered Maxwell model [9] and Fung's viscoelastic model [10] has been used respectively to describe the force response of a "Norimaki-sushi" when grasped by a robot hand. Good approximations of rheological forces were obtained. Unfortunately, both models are 1D cases. In addition, the ISU exoskeleton technique was used to model a clay to simulate interaction between virtual clay and a human finger [11].

However, the above-mentioned works have focused on either reproduction of deformation alone [6], [7] or reproduction of force alone [9], [10]. Nobody considered both of them simultaneously. In many applications, *e.g.*, surgical simulation with haptic feedback or virtual manipulation of food products, accurate results of both force and deformation are necessary. We have therefore focused on the simultaneous reproduction of both rheological deformation and force behaviors.

In this paper, we presented a two-dimensional (2D) FE model for simulating rheological behaviors. Two sets of physical parameters were calculated to capture rheological deformation and force respectively. A parameter switching strategy was then proposed to switch these two sets of parameters during simulation. Experimental results and contact simulations were presented to validate proposed FE model and estimated parameters.

II. MODELING OF RHEOLOGICAL OBJECTS

A. Selection of Physical Model

In our previous work, we have used serial three-element [12], [13], four-element [14], and five-element [15] physical model respectively to describe rheological behaviors. We found that the four-element and five-element models were more appropriate than three-element model for describing rheological forces. We have summarized the physical models, which can be used to simulate rheological behaviors, in [16]. We divided the physical models into two categories: serial and parallel models, as shown in Fig. 1. Both models were

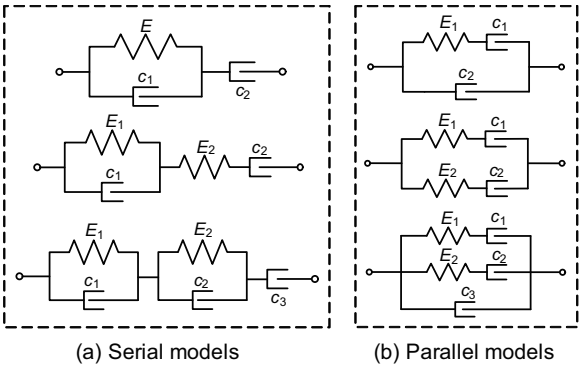

Fig. 1. Two groups of rheological models: (a) serial models; and (b) parallel models.

constructed by a sets of basic elements connected in a serial and parallel configurations. According to the analysis of the constitutive laws, we found that we are always able to find a corresponding parallel model for an arbitrary serial model and both models results in the same rheological behaviors. It means that only one type (either serial or parallel) of rheological model need to be investigated. In this paper, we therefore employed a parallel five-element model (the last row in Fig. 1b) to formulate rheological behaviors.

B. Rheological Force and Deformation

A parallel five-element model consists of two elastic elements (denoted by parameters E_1, E_2) and three viscous elements (denoted by parameters c_1, c_2, and c_3). A elastic element and a viscous element connected in serial was defined as a Maxwell element. Thus, the parallel five-element model also could be described as two Maxwell elements and a viscous element connected in parallel. Let σ_1, σ_2, and σ_3 be the stress at the first, the second Maxwell element, and at the third viscous element, respectively. Let σ and ε be the stress and strain at the 5-element model. The stress-strain relationship can be therefore formulated as:

$$\begin{aligned} &\dot{\sigma}_1 + \frac{E_1}{c_1}\sigma_1 = E_1\dot{\varepsilon}, \\ &\dot{\sigma}_2 + \frac{E_2}{c_2}\sigma_2 = E_2\dot{\varepsilon}, \\ &\sigma_3 = c_3\dot{\varepsilon}, \\ &\sigma = \sigma_1 + \sigma_2 + \sigma_3. \end{aligned} \tag{1}$$

Using finite element (FE) method, we constructed a 2D object with a set of triangles and imposed the five-element model on each triangle to govern the stress-strain relationship. Using generalized Hooke's law, 1D stress-strain relationship Eq. (1) can be convert to a 2D force-displacement relationship as below:

$$\begin{aligned} &\dot{\mathbf{F}}_1 + \frac{E_1}{c_1}\mathbf{F}_1 = (\lambda_1^{ela}\mathbf{J}_\lambda + \mu_1^{ela}\mathbf{J}_\mu)\dot{\mathbf{u}}_N, \\ &\dot{\mathbf{F}}_2 + \frac{E_2}{c_2}\mathbf{F}_2 = (\lambda_2^{ela}\mathbf{J}_\lambda + \mu_2^{ela}\mathbf{J}_\mu)\dot{\mathbf{u}}_N, \\ &\mathbf{F}_3 = (\lambda_3^{vis}\mathbf{J}_\lambda + \mu_3^{vis}\mathbf{J}_\mu)\dot{\mathbf{u}}_N, \\ &\mathbf{F}_{2D}^{rheo} = \mathbf{F}_1 + \mathbf{F}_2 + \mathbf{F}_3, \end{aligned} \tag{2}$$

where $\mathbf{F}_1$, $\mathbf{F}_2$, $\mathbf{F}_3$, and $\mathbf{F}_{2D}^{rheo}$ are force vectors corresponding to stress vectors σ_1, σ_2, σ_3, and σ, respectively. Vector $\mathbf{u}_N$ consists of displacements at individual nodes. Matrices $\mathbf{J}_\lambda$ and $\mathbf{J}_\mu$ are connection matrices which depend only on the distribution of triangular mesh. Let γ be the Poisson's ratio and then variables λ_1^{ela}, μ_1^{ela}, λ_2^{ela}, μ_2^{ela}, λ_3^{vis}, and μ_3^{vis} can be calculated as:

$$\lambda_i^{ela} = \frac{E_i\gamma}{(1+\gamma)(1-2\gamma)}, \quad \mu_i^{ela} = \frac{E_i}{2(1+\gamma)}, \quad (i=1,2),$$
$$\lambda_3^{vis} = \frac{c_3\gamma}{(1+\gamma)(1-2\gamma)}, \quad \mu_3^{vis} = \frac{c_3}{2(1+\gamma)}.$$

C. Boundary Constraints

Supposing that a 2D object was fixed on the ground and the top surface of the object was pushed down with a displacement function of $d(t)$. Therefore, two boundary constraints have to be imposed on the nodes of both top and bottom surfaces. By using constraint stabilization method (CSM) [17], these two boundary constraints can be formulated as:

$$\begin{aligned} \mathbf{A}^T\ddot{\mathbf{u}}_N + \mathbf{A}^T(2\psi\dot{\mathbf{u}} + \psi^2\mathbf{u}_N) = 0, \\ \mathbf{B}^T(\ddot{\mathbf{u}}_N - \ddot{\mathbf{d}}) + \mathbf{B}^T[2\psi(\dot{\mathbf{u}}_N - \dot{\mathbf{d}}) + \psi^2(\mathbf{u}_N - \mathbf{d})] = 0, \end{aligned} \tag{3}$$

where matrix $\mathbf{A}$ and $\mathbf{B}$ denotes the nodes should be constrained on both top and bottom surfaces. Scalar ψ was a predetermined angular frequency and was set to 2000 for both constraints.

D. 2D FE Dynamic Equations

Let $\mathbf{M}$ be the inertia matrix and λ_1 and λ_2 be the Lagrange multipliers which denote a set of constraint forces corresponding to both boundary constraints. Using the Lagrange dynamic method, dynamic equations of all nodes are formulated as

$$-\mathbf{F}_{2D}^{rheo} + \mathbf{A}\lambda_1 + \mathbf{B}\lambda_2 - \mathbf{M}\ddot{\mathbf{u}}_N = 0. \tag{4}$$

Combining Eqs. (2), (3), (4), and considering $\mathbf{v}_N = \dot{\mathbf{u}}_N$, we could end up with a set of differential equations which described the 2D dynamic behaviors of a rheological object under a pushing or pulling operation. By numerically solving these equations, we could calculate the deformation and forces at each nodes of the triangular mesh. In addition, the 2D FE model can be easily extended to 3D case by changing the triangular mesh to tetrahedral mesh and adding the z-axis components in all the matrices and vectors.

III. PARAMETER ESTIMATION

A. Analytical Expressions of Forces

Generally, the properties of various materials were estimated through some standard compressive or tensile tests. Mostly, such tests only provided 1D measurement data. In our applications, however, 2D/3D measurements are required. We pushed a flat-squared object from the entire top surface with a constant velocity from time 0 to t_p and this time period was called pushing phase. Before releasing the deformation, the deformed shape was maintained from time t_p to $t_p + t_k$ and this period was called keep phase. During the

compressive test, the force responses and several deformed images were recorded by a tactile sensor and a calibrated camera. Using these experimental measurements, we were able to estimate the physical parameters.

We previously proposed an approach to estimate the parameters based on FE simulation and iterative optimization. The idea of this method is to iterate the FE simulation with updated physical parameters until the difference between the simulation and experiment becomes minimal. This method was robust but time consuming. Therefore in this paper, we introduced an efficient method to estimate the rheological properties by taking the advantages of analytical expressions of rheological forces. Note that the pushing velocity is constant in pushing phase and is zero in the keep phase. Therefore, we can easily solve the differential equations of Eq. (2) in both pushing and keep phase. Finally, we have the expressions of rheological forces in both phases as follows:

$$\mathbf{F}(t) = \sum_{i=1}^{2} c_i\big(1-e^{-\frac{E_i}{c_i}t}\big)\mathbf{M}_\gamma\mathbf{p} + c_3\mathbf{p},\ (0 \le t \le t_p), \quad (5)$$

$$\mathbf{F}(t) = \sum_{i=1}^{2} c_i\big(1-e^{-\frac{E_i}{c_i}t_p}\big)e^{-\frac{E_i}{c_i}(t-t_p)}\mathbf{M}_\gamma\mathbf{p},\ (t_p \le t \le t_p+t_h), \quad (6)$$

where

$$\mathbf{M}_\gamma = \gamma_\lambda\mathbf{J}_\lambda + \gamma_\mu\mathbf{J}_\mu = \frac{\gamma}{(1+\gamma)(1-2\gamma)}\mathbf{J}_\lambda + \frac{1}{2(1+\gamma)}\mathbf{J}_\mu.$$

Vector $\mathbf{p}$ consists of velocities at individual nodes in the pushing phase. Note that the Poisson's ratio γ can be determined in advance by using the experimental data of deformed shape in the keep phase, as discussed in [17]. The vector $\mathbf{p}$ can be then obtained from the simulation results during pushing operation with known γ. Using Eqs. (5) and (6), we can easily calculate the force responses during both pushing and keep phases.

B. Analytical Expression of Residual Deformation

According to the discussions of our previous work [16], we found that the residual deformation was dominated by the sum of the viscous moduli $\sum_1^3 c_i$ and force history through pushing and keep phases. The residual deformation $\mathbf{u}_N(\infty)$ can be formulated as:

$$\mathbf{M}_\gamma\mathbf{u}_N(\infty) = \frac{1}{\sum_{i=1}^3 c_i}\int_0^{t_p+t_k}\mathbf{F}(t)\mathrm{d}t. \quad (7)$$

C. Parameter Estimation

Using Eqs. (5) and (6), we can estimate parameters E_1, E_2, c_1, c_2, and c_3 by minimizing the force difference during pushing and keep phase. Instead of using iterative FE simulation, we calculated all the force data directly from the force expressions. This method could result in an optimized solution within only several seconds depended on the initial setting. The estimated parameters from this optimization provided accurate force results but we failed to reproduce residual deformation. In order to accurately capture residual deformation, the sum of the viscous moduli $\sum_1^3 c_i$ has to be close to the value calculated from Eq. 7. If we predetermined the value of $\sum_1^3 c_i$ and used it as a constraint to minimize the force difference, we could estimate all the parameters and yield a good reproduction of residual deformation. Again, we were not able to accurately reproduce the force response at the same time. We therefore concluded this behavior as a contradiction between accurate reproduction of force response and reproduction of residual deformation. This behavior only happens in rheological object where the residual deformation exists. This is because the physical model used in our FE formulation is a linear model, especially the linear viscous element. We found that this contradiction phenomenon will appear as long as the physical model is linear and no matter how many elements included in the physical model. However, we could employ two sets of parameters to capture force and deformation respectively, as discussed in [17]. The estimation process of two sets of parameters can be summarized as the following four steps:

1) Estimation of Poisson's ratio γ by minimizing the difference of deformed shape in keep phase;
2) Estimation of the first set parameters by minimizing the force difference based on Eqs. (5) and (6);
3) Calculating the value of $\sum_1^3 c_i$ using Eq. (7).
4) Estimation of the second set parameters by minimizing the force difference with known $\sum_1^3 c_i$ as a constraint.

D. Parameter Switching Strategy

As discussed in the last section, two sets of parameters were necessary to accurately reproduce both rheological force and deformation. We could use both sets of parameters as input to simulate the rheological objects, as presented in [17]. However, this is time-consuming since two geometrically identical objects need to be simulated inside the simulator. In this paper, we therefore proposed a parameter switching strategy to switch these two sets of parameters from one set to the other. As shown in Eq. 7, since the residual deformation was dominated by $\sum_1^3 c_i$, we have therefore proposed a dual-moduli viscous element as shown in Fig. 2a. The stress-strain relationship of the dual-moduli viscous element was formulated as:

$$\sigma(t) = (\kappa\alpha + c)\dot{\varepsilon}(t), \quad (8)$$

where scalars α and c were parameters to be determined. Switch function κ takes the following value:

$$\kappa = \begin{cases} -1 & \text{criterion is satisfied;} \\ 1 & \text{otherwise.} \end{cases} \quad (9)$$

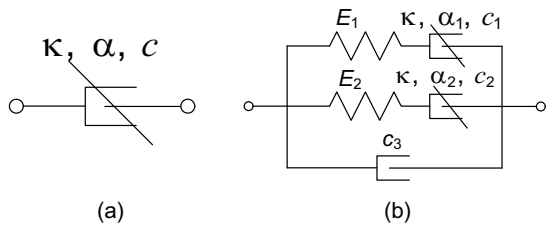

Fig. 2. (a) the dual-moduli viscous element and (b) parallel 5-element model with two dual-moduli viscous elements.

TABLE I

ESTIMATED PARAMETERS FOR BOTH MATERIALS

Material	γ	E_1 (Pa)	E_2 (Pa)	c_1 (Pa·s)	c_2 (Pa·s)	α_1 (Pa·s)	α_2 (Pa·s)
Clay	0.2902	3.7731×10^4	8.0952×10^4	1.1247×10^7	5.9559×10^5	2.0444×10^6	1.0179×10^5
Sweets	0.3474	1.3787×10^4	2.5865×10^4	2.7672×10^7	6.0402×10^4	2.7657×10^7	6.4650×10^3

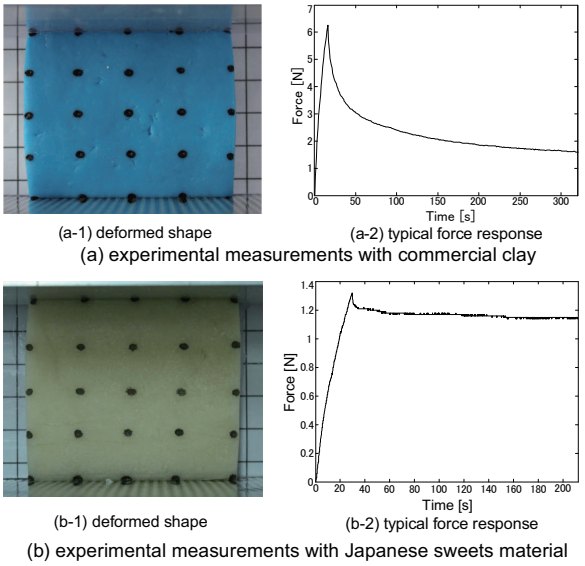

Fig. 3. deformed shapes and typical force responses of both commercial clay and Japanese sweets material.

Introducing two dual-moduli viscous elements into the parallel 5-element model, as shown in Fig. 2b, we could modify the FE model by replacing the first two equations of Eq. (2) with the following two equations:

$$\begin{aligned} \dot{\mathbf{F}}_1 + \frac{E_1}{\kappa\alpha_1 + c_1}\mathbf{F}_1 &= (\lambda_1^{ela}\mathbf{J}_\lambda + \mu_1^{ela}\mathbf{J}_\mu)\dot{\mathbf{u}}_N, \\ \dot{\mathbf{F}}_2 + \frac{E_2}{\kappa\alpha_2 + c_2}\mathbf{F}_2 &= (\lambda_2^{ela}\mathbf{J}_\lambda + \mu_2^{ela}\mathbf{J}_\mu)\dot{\mathbf{u}}_N. \end{aligned} \tag{10}$$

The parameter switching should happen in the moment when the deformation started to recover. Thus, the criterion used in Eq. 9 could be time or some events which can easily distinguish the recovery moment. In the rest of this paper, we will introduce two such criterions: simulation time and contact detection.

IV. EXPERIMENTS AND VALIDATION

A. Experimental Results and Estimated Parameters

Two rheological objects made of commercial available clay and Japanese sweets material were used in our experiments. The flat-squared objects were pushed with a constant velocity of 0.2 m/s by a linear stage. Some markers were drawn on the object surfaces for easy comparison of internal deformation. The force responses were measured by a tactile sensor. Initial, deformed, and recovered shapes were recorded by a calibrated camera. Deformed shapes of both materials

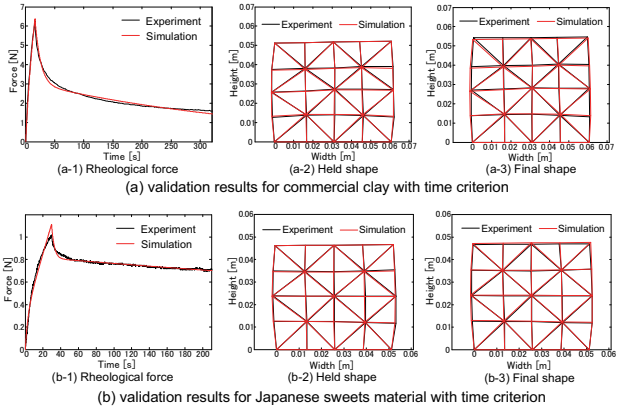

Fig. 4. Validation results of both materials with the time criterion.

and the typical force responses were shown in Fig. 3. These measured data were then used to estimate the physical parameters and the estimated results for both materials were given in Table I.

B. Validation Results

1) Validation with Time Criterion: Using the proposed FE model and estimated parameters, we could simulate the behaviors of above two objects. At first, we used simulation time as a criterion to start the parameter switching. The simulation results compared with experimental measurements were demonstrated in Fig. 4. We were able to accurately reproduce both rheological forces and deformation simultaneously.

2) Validation with Criterion of Contact Detection: Contact between an object and an external instrument often happens in many applications, such as surgery operation and food grasping. During the contact modeling, we found that the moment of losing contact could serve as a good criterion for parameter switching. The process of contact modeling was presented in [18]. Using the estimated parameters of sweets material (as listed in Table I), we performed a contact simulation between a rheological object and an external instrument. The simulation results compared with experimental measurements were shown in Fig. 5. We successfully reproduced both rheological force and deformation behaviors by using the proposed parameter switching strategy.

We also conducted simulations with irregular shaped objects. For example, a semi-circular object was deformed by a squared instrument. Total simulation time is 16 seconds. The instrument was moved down 25 mm in first 4 seconds with a constant velocity. Then, the instrument was stopped

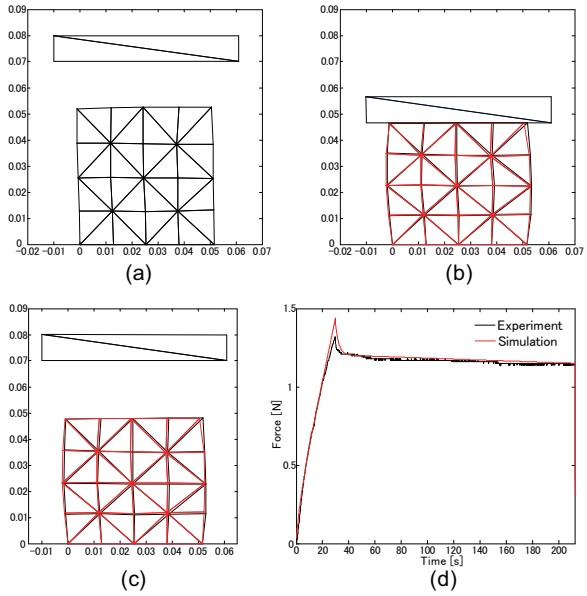

Fig. 5. Validation results of Japanese sweets material with criterion of contact detection. Simulation results (red line) compared with experimental measurements (black line): (a) the initial shape and position of the object and instrument, (b) the deformed shape when the deformation was holding, (c) the final recovered shape, and (d) the rheological force behaviors.

and maintained the deformed object for 4 seconds. The instrument moved back to the original position within another 4 seconds. After the instrument was moved back to the original position, the object still had 4 seconds to recover. The estimated parameters of sweets material were used in this simulation. Some snapshots of simulation results were shown in Fig. 6, where the parameter switching strategy was applied. To demonstrate the function of parameter switching strategy, snapshots without parameter switching were also given in Fig. 7. In this case, we could obtain accurate force results but the deformation behaviors were not as we expected. At simulation time 8.2 s, the instrument and object had lost contact in Fig. 6d but still in contact in Fig. 7a. The final recovered shapes of both cases were also quite different.

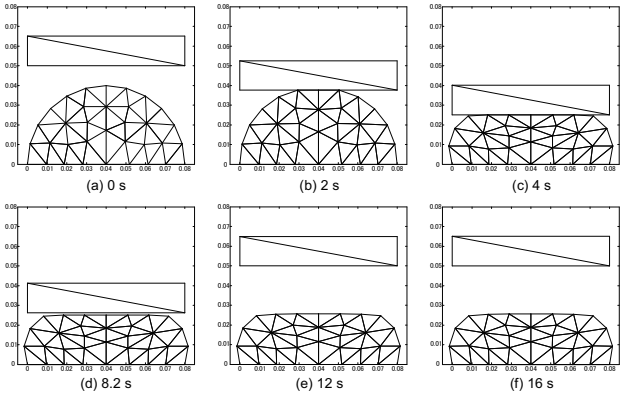

Fig. 6. Simulation snapshots of a semi-circular object pushed down by a flat squared instrument with parameter switching strategy.

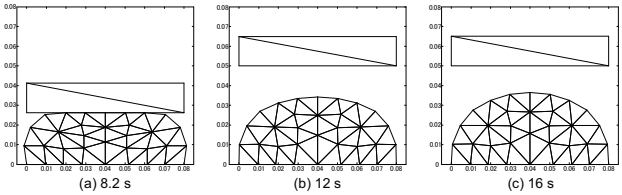

Fig. 7. Simulation snapshots without parameter switching.

In addition, we also investigated the rheological behaviors of a circular object operated by two external instruments with one at the top and the other at the bottom, as shown in Fig. 8 with parameter switching and in Fig. 9 without parameter switching. The bottom instrument was static and the top instrument was moved down to push the object. Figure 8b showed that the object had already deformed and contacted with the bottom instrument due to gravity before the top instrument touch the object. The final recovered shape was also not symmetrical relative to the horizontal axis due to the gravity in both figures. The deformation behaviors showed that our FE model worked in a natural way.

V. CONCLUSIONS AND FUTURE WORKS

In this paper, a parallel five-element physical model was used to describe the rheological behaviors and a 2D/3D FE dynamic model were formulated to simulate such behaviors. By taking the advantage of parallel configuration of the five-element model, analytical expressions of rheological force and residual deformation were formulated and an efficient approach for estimating physical parameters was then presented based on these expressions and nonlinear optimizations. To accurately reproduce both rheological deformation and force simultaneously, two sets of physical parameters were estimated. One of each captures deformation and force respectively. A parameter switching strategy was then proposed to switch these parameters from one

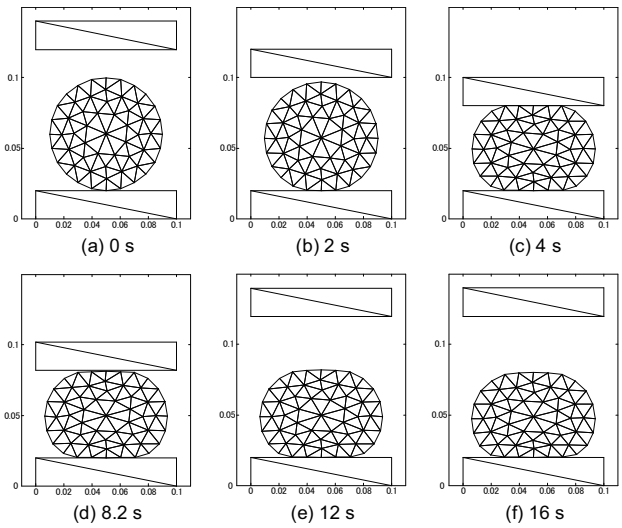

Fig. 8. Simulation snapshots of a circular object operated by two instruments with parameter switching strategy.

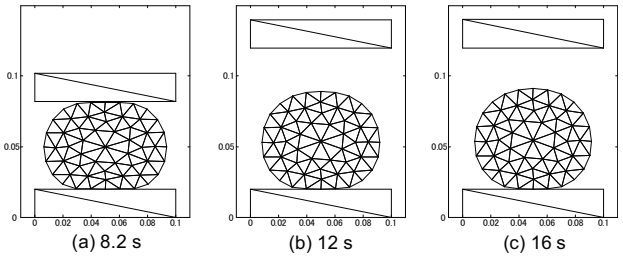

Fig. 9. Simulation snapshots of a circular object operated by two instruments without parameter switching strategy.

set to another when a criterion was satisfied. Experimental results using commercial available clay and Japanese sweets materials were given to validate proposed FE model and estimated parameters. Finally, contact simulations between rheological objects and external instruments were presented to demonstrate the ability of our FE model for dealing with arbitrary shaped objects.

In the future, nonlinear modeling, such as geometrical nonlinearity, will be introduced into our FE model to cover large deformation and rotation behaviors. In addition, more rheological materials, including biological organs or tissues, will be tested to further validate our FE model and parameter estimation method.

VI. ACKNOWLEDGMENTS

This research is supported in part by Grant in Aid for Scientific Research (No. 20246049) and R-GIRO program of Ritsumeikan University.

REFERENCES

[1] D. Terzopoulos, J. Platt, A. Barr, and K. Fleischer, "Elastically deformable models", *Proc. 14th Annual Conference on Computer Graphics and Interactive Techniques (SIGGRAPH '87)*, pp. 205–214, Anaheim, 1987.

[2] D. Terzopoulos and K. Fleischer, "Modeling inelatic deformation: viscoelasticity, plasticity, fracture", *Proc. 15th Annual Conference on Computer Graphics and Interactive Techniques (SIGGRAPH '88)*, pp. 269–278, Atlanta, 1988.

[3] M. Hrapko, J.A.W. van Dommelen, G.W.M. Peters, and J.S.H.M. Wismans, "The mechanical behaviour of brain tissue: Large strain response and constitutive modelling", *Biorheology*, vol. 43, pp. 623–636, 2006.

[4] A. Nava, E. Mazza, M. Furrer, P. Villiger, and W.H. Reinhart, "In vivo mechanical characterization of human liver", *Med. Image Anal.*, vol. 12, pp. 203–216, 2008.

[5] P.Y. Chua, T. Ilschner, and D.G. Caldwell, "Robotic manipulation of food products—a review", *Ind. Robot*, vol. 30, No. 4, pp. 345–354, 2003.

[6] H. Yoshida, Y. Murata, and H. Noborio, "A Smart Rheologic MSD Model Pushed/Calibrated/Evaluated by Experimental Impulses," *Proc. IEEE/RSJ International Conference on Intelligent Robots and Systems (IROS '05)*, pp. 269–276, Edmonton, 2005.

[7] T. Ikawa and H. Noborio, "On the Precision and Efficiency of Hierarchical Rheology MSD Model," *Proc. IEEE/RSJ International Conference on Intelligent Robots and Systems (IROS '07)*, pp. 376–383, San Diego, 2007.

[8] B. A. Lioyd, G. Székely, and M. Harders, "Identification of spring parameters for deformable object simulation," *IEEE Trans. Vis. Comput. Graph.*, vol.13, no.5, pp. 1081–1094, Sept./Oct., 2007.

[9] N. Sakamoto, M. Higashimori, T. Tsuji, and M. Kaneko, "An Optimum Design of Robotic Hand for Handling a Visco-elastic Object Based on Maxwell Model," *Proc. IEEE International Conference on Robotics and Automation (ICRA '07)*, pp. 1219–1225, Roma, 2007.

[10] C.-H.D. Tsai, I. Kao, N. Sakamoto, M. Higashimori, and M. Kaneko, "Applying Viscoelastic Contact Modeling to Grasping Task: An Experimental Case Study," *Proc. IEEE/RSJ International Conference on Intelligent Robots and Systems (IROS '08)*, pp. 1790–1795, Nice, 2008.

[11] Y.-H. Chai, G. R. Luecke, and J. C. Edwards, "Virtual Clay Modeling Using the ISU Exoskeleton," *Proc. IEEE Virtual Reality Annual International Symposium (VRAIS '98)*, pp. 76–80, Atlanta, 1998.

[12] J. Muramatsu, T. Ikuta, S. Hirai, and S. Morikawa, "Validation of FE deformation models using ultrasonic and MR images," in *Proc. 9th International Conference on Control, Automation, Robotics and Vision (ICARCV'06)*, pp. 1–6, Singapore, 2006.

[13] Z. Wang, K. Namima, and S. Hirai, "Physical parameter identification of rheological object based on measurement of deformation and force," *Proc. IEEE International Conference on Robotics and Automation (ICRA '09)*, pp. 1238–1243, Kobe, 2009.

[14] Z. Wang and S. Hirai, "Modeling and parameter identification of rheological object based on FE method and nonlinear optimization," *Proc. IEEE/RSJ International Conference on Intelligent Robots and Systems (IROS '09)*, pp. 1968–1973, St. Louis, 2009.

[15] Z. Wang and S. Hirai, "Modeling and property estimation of Japanese sweets for their manufacturing simulation," *Proc. IEEE/RSJ International Conference on Intelligent Robots and Systems (IROS '10)*, Taipei, 2010, accepted.

[16] Z. Wang and S. Hirai, "Modeling and parameter estimation of rheological objects for simultaneous reproduction of force and deformation," in *1st International Conference on Applied Bionics and Biomechanics (ICABB2010)*, Venice, 2010, accepted.

[17] Z. Wang and S. Hirai, "Modeling and estimation of rheological properties of food products for manufacturing simulations," *Journal of Food Engineering*, 2010, doi:10.1016/j.jfoodeng.2010.08.011.

[18] Z. Wang and S. Hirai, "Contact modeling and parameter switching for simultaneous reproduction of rheological force and deformation," *Proc. IEEE International Conference on Robotics and Biomimetics (ROBIO2010)*, 2010, submitted.